JOURNAL OF GEOPHYSICAL RESEARCH, VOL. 111, F03015, doi:10.1029/2006JF000477, 2006

An evaluation of the geomorphically effective event for fluvial processes over long periods

Xiangjiang Huang[1] and Jeffrey D. Niemann[2]

Received 2 February 2006; revised 8 May 2006; accepted 2 June 2006; published 19 September 2006.

[1] Fluvial processes erode landscapes in response to a wide range of discharges. The importance of a given discharge to the erosion of a basin can be calculated by multiplying the discharge's frequency of occurrence and the erosion rate produced by the discharge. The discharge that contributes the most geomorphic work is called the geomorphically effective event (GEE). In this paper, the behavior of the GEE is examined when a generic stream power model with a threshold is used to describe either the detachment or transport of sediment by flowing water. The results suggest that the return period of the GEE depends primarily on the threshold value when the exponent on discharge is less than 2. Otherwise, it depends primarily on the exponent. The GEE usually cannot be substituted for the probability density function of discharge because it produces a different long-term erosion rate. Furthermore, the return period of the GEE can vary spatially in a basin. For example, the return period can be different between locations where the fluvial process is dominant and subdominant if the threshold is nonzero. For a detachment-limited model the return period of the GEE is different upstream and downstream of knickpoints, and for a transport-limited model the return period is different along channel profiles even at steady state. Spatial variation in streamflow generation also produces spatial variations in the return period of the GEE.

Citation: Huang, X., and J. D. Niemann (2006), An evaluation of the geomorphically effective event for fluvial processes over long periods, *J. Geophys. Res.*, *111*, F03015, doi:10.1029/2006JF000477.

1. Introduction

[2] Over long periods, landscapes respond to fluvial processes driven by a wide range of discharges. Low discharges have little ability to modify the land surface, but this contribution is magnified because such flow rates are common. High discharges have a much greater ability to modify the land surface but rarely occur. The concept of a geomorphically effective event (GEE) was proposed by *Wolman and Miller* [1960], who suggested that the geomorphic work done by a particular discharge can be measured by the product of the sediment transport rate that occurs as a result of the discharge and the frequency with which the discharge recurs. The GEE is the event that maximizes this product and is also termed the effective discharge. On the basis of their observations, the GEE for suspended sediment load is a relatively frequent event occurring about once a year. Numerous subsequent researchers repeated this magnitude-frequency analysis for other streams, and these results show that the return period of the GEE is highly variable between locations [e.g., *Benson and Thomas*, 1966; *Andrews*, 1980; *Nolan et al.*, 1987; *Ashmore and Day*, 1988; *Leopold*, 1994; *Sichingabula*, 1999]. *Kirchner et al.* [2001] used isotopic techniques to measure sediment yield over large timescales in 32 mountain catchments in Idaho and found that the long-term sediment yield is dominated by rare catastrophic erosion events instead of the frequent erosion events. *Ashmore and Day* [1988] studied suspended sediment transport and streamflow for 21 streams in the Saskatchewan basin and found it impossible to make a generalization about the return period of the GEE. In order to explain the variability of the observed effective discharge, *Wolman and Gerson* [1978], *Ritter* [1988], and *Miller* [1990] suggested that the effectiveness of discharges in removing sediment in rivers is not necessarily equivalent to effectiveness in shaping the landscape as a whole, implying that sediment transport is just one of many relevant fluvial processes. *Hartshorn et al.* [2002] examined the impact of event sizes on bedrock incision along a channel cross section in Taiwan and found that vertical incision is driven by frequent events, while rare events associated with supertyphoons play a role in widening the channel.

[3] The return period of the GEE can also vary between upstream and downstream locations if the frequency of occurrence of discharge and fluvial processes are scale-dependent. *Wolman and Miller* [1960] suggested that the skewness of the distribution of discharges decreases with increasing basin area, which would cause a decreasing return period for the GEE as one moves downstream. This result is supported by the study of *Andrews* [1980] who

[1]Department of Civil and Environmental Engineering, Pennsylvania State University, University Park, Pennsylvania, USA.
[2]Department of Civil Engineering, Colorado State University, Fort Collins, Colorado, USA.

0148-0227/06/2006JF000477$09.00

estimated the effective discharges at 15 gauging stations and found that the return period of the GEE decreases with increasing basin area.

[4] The GEE has also been considered from a more theoretical standpoint. *Nash* [1994] studied the GEE by assuming lognormally distributed discharges and a power law relationship between sediment transport rate and discharge, and he compared the predicted GEE values with estimates for 55 U.S. streams. The theoretical analysis shows that the GEE increases exponentially with an increasing exponent on discharge in the sediment transport model and that the return period of the GEE increases with discharge variability. However, he also found that the observed and predicted return periods of the GEE are in poor agreement due to the failure of the power law function to predict accurately sediment transport rates, perhaps due to the presence of thresholds. *Baker* [1977] noted earlier that thresholds for erosion models tend to shift the GEE to larger and less common events. *Costa and O'Connor* [1995] considered the fact that discharge varies during any given hydrograph. If a threshold is present, they argued that the geomorphic effectiveness of the hydrograph is determined by the combination of a large peak discharge and a long duration during which the discharge exceeds the threshold.

[5] Although the determination of the GEE is complicated by the factors described above, the GEE is used in many applications, such as stream restoration [*Shields et al.*, 2003] and the evaluation of ecological processes [*Doyle et al.*, 2005]. The concept of an effective discharge is also a valuable tool in analyzing and modeling geomorphic processes because it allows one to quantify the role of discharge and sometimes climate with few variables or parameters. For example, in field studies of geomorphic processes, the effectiveness of fluvial processes is commonly quantified using drainage area as a substitute for discharge [e.g., *Montgomery and Dietrich*, 1992; *Roering et al.*, 1999]. This approach implicitly represents fluvial processes by an effective discharge, which is assumed to depend linearly on drainage area with some unknown coefficient. Similarly, numerical landscape evolution models simulate bedrock detachment and/or sediment transport caused by flowing water as a function of an effective discharge [e.g., *Kirkby*, 1986, 1987; *Willgoose et al.*, 1991a, 1991b, 1991c; *Anderson*, 1994; *Howard*, 1994, 1997, 1999; *Tucker and Slingerland*, 1994, 1997; *Densmore et al.*, 1998; *Whipple and Tucker*, 1999]. In such models, the fluvial processes occur in response to either a perpetual or intermittent effective discharge [*Paola et al.*, 1992; *Tucker and Slingerland*, 1997; *Howard*, 1999]. However, it is not clear that these effective discharges are equivalent to the GEE. Some recent landscape evolution modeling studies have discarded the effective discharge in favor of a stochastic model for precipitation events [e.g., *Tucker and Bras*, 2000]. In order to examine the role of extreme discharges in fluvial erosion, *Lague et al.* [2005] assumed that the distribution of daily discharges has a power law tail instead of the exponential tail, and found that discharge variability has a complex effect on the predicted steady state river profile.

[6] In this study, we seek to understand the behavior of GEE for stream power models when a threshold is included. In particular, what characteristics of the model control the GEE? Is the GEE equivalent to the effective discharge? Do we expect the GEE to be the same among different fluvial processes? Do we expect the GEE to have the same return period throughout a basin? We first extend the analytical analysis of *Nash* [1994] by introducing thresholds in the representations of the fluvial processes and investigating the impacts on the GEE (section 2). Then, we use a 1-D numerical model to simulate the evolution of a combined hillslope and river profile (section 3). In this model, precipitation events are generated using the Poisson rectangular pulse model [*Eagleson*, 1978; *Tucker and Bras*, 2000], and the GEE is estimated for both detachment-limited and transport-limited conditions along the river profiles during steady state and transient states. Finally, we use a 2-D detachment-limited landscape evolution model to consider the role of runoff generation mechanisms in determining the GEE (section 4). We simulate groundwater movement using a dynamic 2-D Dupuit equation for a homogeneous, isotropic, and unconfined aquifer [*Huang and Niemann*, 2006]. Our main conclusions are highlighted in section 5.

2. Analytical Analysis

2.1. Determining the GEE of a Fluvial Process

[7] For any location on a landscape, the strength of a fluvial process can be viewed as a random variable in time, which we denote as E. E could represent the rate of fluvial detachment of bedrock or the sediment transport rate, but for simplicity we refer to it as an erosion rate. Because E is a continuous random variable, the frequency with which a given value of E occurs can be described by a probability density function (PDF) $f_E(E)$. If $f_E(E)$ is known, then the mean erosion rate $\overline{E}$ can be found from:

$$\overline{E} = \int_0^\infty E f_E(E) dE. \tag{1}$$

E is not usually considered an independent variable; rather, it is a function of the discharge Q. So, one can write $E = g(Q)$, where g describes the dependence of the erosion on discharge, and the discharge Q is the random variable that is determined independently. If we know the PDF of discharge $f_Q(Q)$ and assume g to be a monotonically increasing function, then $f_E(E)$ can be derived using the well-known derived distribution formula [*Ang and Tang*, 1975]:

$$f_E(E) = f_Q\left(g^{-1}(E)\right) \frac{dg^{-1}(E)}{dE}. \tag{2}$$

Substituting this relationship into equation (1), one can also calculate the mean erosion rate as:

$$\overline{E} = \int_0^\infty g(Q) f_Q(Q) dQ \tag{3}$$

or in the more common notation:

$$\overline{E} = \int_0^\infty E f_Q(Q) dQ. \tag{4}$$

The contribution of a range of discharges to the mean erosion rate can be calculated by restricting the integration in equation (4):

$$\int_{Q_1}^{Q_2} Ef_Q(Q)dQ \tag{5}$$

where Q_1 and Q_2 define the range of interest. If one considers smaller ranges of discharge, it becomes clear that $Ef_Q(Q)$, despite its peculiar units, is a measure of the importance of a given discharge Q to the mean erosion rate. The discharge with the largest value of $Ef_Q(Q)$ is the most important discharge to the evolution of the landscape and is usually considered as the GEE [e.g., *Wolman and Miller*, 1960; *Nash*, 1994]. We refer to this discharge as Q_p, where the subscript "p" indicates it is the primary discharge to which the landscape responds. It should be noted that alternative definitions for the GEE have been proposed in the literature including the discharge associated with the median of $Ef_Q(Q)$ [*Vogel et al.*, 2003].

[8] In order to evaluate the GEE, a generic expression relating discharge and the fluvial erosion rate is considered. In particular, we use

$$E = \beta Q^m S^n - \Phi \tag{6}$$

where β is an erodability coefficient, S is the local slope, m and n are constant exponents, and Φ is a threshold that must be exceeded before erosion occurs. This type of model is commonly referred to as the stream power model, and it has been used to describe the fluvial detachment of bedrock and the transport of sediment [e.g., *Howard*, 1994; *Tucker and Slingerland*, 1997]. The stream power model can be derived from several conceptual views of erosion. For example, *Howard and Kerby* [1983] suggested that the detachment rate of bedrock is proportional to shear stress, which depends on the hydraulic radius of the channel and the local slope and can be expressed in a form like equation (6). *Seidl and Dietrich* [1992] presented another model for bedrock detachment where bedrock incision is proportional to the stream power, which is the product of discharge and slope. As for sediment transport capacity, many of the commonly used sediment transport equations can be recast into a power law function of discharge and slope [*Willgoose et al.*, 1991a; *Howard*, 1994]. However, equation (6) excludes some important models of bedrock detachment [e.g., *Sklar and Dietrich*, 1998; *Whipple and Tucker*, 1999] and sediment transport [e.g., *Bagnold*, 1954]. The exponent m for bedrock detachment usually ranges from 1/3 to 5/6, which depends upon bedrock erosion processes [*Hancock et al.*, 1998]. The exponent m for sediment transport is usually larger than one, for example, 1.5 [*Howard*, 1994]. The ratio m/n for bedrock detachment is found to fall into a relatively narrow range near 0.5, consistent with empirical values derived from field data [*Whipple and Tucker*, 1999]. For the sake of mathematical convenience, a critical discharge Q_c can be defined as

$$Q_c = \left(\frac{\Phi}{\beta S^n}\right)^{1/m} \tag{7}$$

which allows equation (6) to be written as

$$E = \beta S^n \left(Q^m - Q_c^m\right). \tag{8}$$

Notice that the critical discharge Q_c has an inverse relationship with slope, so one could also express the threshold in terms of a critical slope.

[9] To determine the GEE, the PDF of discharge also needs to be identified. We consider two PDFs: the one-parameter exponential distribution and two-parameter lognormal distribution. The exponential distribution has been used previously in landscape evolution modeling because of its simplicity. *Tucker and Bras* [2000] simulated precipitation as a series of storm events that occur according to the Poisson rectangular pulse model [*Eagleson*, 1978]. In this model, the rainfall rate during a storm P, the storm duration T_r, and the time between consecutive storms T_o are all considered as independent random variables. Each variable conforms to an exponential distribution, so for example the PDF for rainfall rate P is

$$f_P(P) = \frac{1}{\overline{P}} \exp\left(-\frac{P}{\overline{P}}\right) \tag{9}$$

where $\overline{P}$ is the mean rainfall rate when rain is occurring. If the watershed or region under consideration is relatively small, then the rainfall rate is approximately constant in space and the response time of the basin is shorter than the duration of the storm event. If the infiltration rate is neglected, then all precipitation becomes surface runoff and the discharge Q at any channel cross section can be found from

$$Q = PA \tag{10}$$

where A is the land area that drains through the cross section. Thus the PDF of the discharge during storm events is

$$f_Q(Q) = \frac{1}{\overline{Q}} \exp\left(-\frac{Q}{\overline{Q}}\right) \tag{11}$$

where the mean discharge during a storm is $\overline{Q} = \overline{P}A$ [*Tucker and Bras*, 2000]. The PDF for discharge is fully defined if we known either $\overline{Q}$ or $\overline{P}$. Notice that the average discharge during the year is much lower than $\overline{Q}$ due to the large periods between storms in which discharge is assumed to be zero. The mean value of the annual discharge $\overline{Q}_{annual}$ can be found:

$$\overline{Q}_{annual} = \frac{\overline{T}_r}{\overline{T}_r + \overline{T}_o}\overline{Q}. \tag{12}$$

where $\overline{T}_r$ is the mean storm duration and $\overline{T}_o$ is the mean interstorm period.

[10] The lognormal distribution is often used to represent the PDF of daily discharges for perennial channels [*Chow*, 1954; *Krumbein*, 1955; *Kuczera*, 1982; *Leopold*, 1994]. Here, this distribution is used to describe the discharge during storm events across the small watershed or landscape. Because the lognormal distribution includes two

parameters, it allows explicit consideration of the role of the variance in determining the GEE. The lognormal PDF for discharge can be written as

$$f_Q(Q) = \frac{1}{Q\sqrt{2\pi}\sigma_y} \exp\left[-\frac{1}{2}\left(\frac{\ln(Q)-\mu_y}{\sigma_y}\right)^2\right] \quad (13)$$

where $y \equiv \ln(Q)$, and μ_y and σ_y are the mean and standard deviation of y, respectively. μ_y and σ_y can be calculated from:

$$\mu_y = \ln\left(\frac{\overline{Q}}{\sqrt{1+C_Q^2}}\right) \quad (14)$$

$$\sigma_y^2 = \ln\left(1+C_Q^2\right) \quad (15)$$

where $\overline{Q}$ and C_Q are the mean and coefficient of variation (the standard deviation divided by the mean) of the discharge during storms, respectively. A larger value for σ_y (or C_Q) leads to a larger skewness of the distribution and a longer tail on the PDF of discharge, which emphasizes the importance of extreme events in fluvial processes. It should be noted that other distributions have been proposed for discharge. *Lague et al.* [2005] used a distribution of discharge characterized by a power law tail instead of the exponential tail to investigate the effects of discharge variability on river profiles. Recently, *Molnar et al.* [2006] observed that the frequency of extreme discharges obeys a distribution with a power law tail for numerous gages across the US.

[11] We first use the exponential distribution to calculate the GEE for a single fluvial process that conforms to the stream power model (either fluvial detachment or sediment transport capacity). Recall that the geomorphic effectiveness of a given discharge Q is the product $Ef_Q(Q)$, which for the stream power model and exponential distribution is

$$Ef_Q(Q) = \frac{\beta S^n}{\overline{Q}}\left(Q^m - Q_c^m\right)\exp\left(-\frac{Q}{\overline{Q}}\right). \quad (16)$$

Taking the derivative of $Ef_Q(Q)$ with respect to Q and setting it equal to zero leads to the implicit expression for the GEE (Q_p):

$$Q_p^m - m\overline{Q}Q_p^{m-1} - Q_c^m = 0 \quad (17)$$

where this solution requires $Q_p > Q_c$. For the simple case where $Q_c = 0$, Q_p has the simplified and explicit form:

$$Q_p = m\overline{Q} \quad (18)$$

which implies that, even when a threshold is absent, the most important discharge is not the mean discharge if the model is nonlinear. It also implies that variability in the discharge has a first-order effect on the rate of the fluvial process, meaning that the mean rate of the fluvial process depends on the variability of the discharge. This tendency becomes clearer if the lognormal distribution is used to describe discharge. In this case, the geomorphic effectiveness $Ef_Q(Q)$ is

$$Ef_Q(Q) = \frac{\beta S^n}{\sqrt{2\pi}\sigma_y}\left(Q^{m-1} - Q_c^m Q^{-1}\right)\exp\left[-\frac{1}{2}\left(\frac{\ln(Q)-\mu_y}{\sigma_y}\right)^2\right]. \quad (19)$$

Again, taking the derivative of this expression with respect to Q and setting it equal to zero leads to the implicit expression for the GEE:

$$\frac{\ln(Q_p)-\mu_y}{\sigma_y^2} = m - 1 + \frac{mQ_c^m}{Q_p^m - Q_c^m} \quad (20)$$

where this solution applies for $Q_p > Q_c$. If $Q_c = 0$, Q_p has the explicit form:

$$Q_p = \overline{Q}\cdot\left(C_Q^2+1\right)^{m-3/2}. \quad (21)$$

The first term on the right side of this equation is the mean of discharge for the lognormal distribution (see equation (14)) and the second term indicates that the GEE increases with increasing discharge variability C_Q [*Nash*, 1994; *Vogel et al.*, 2003]. Equation (18) for the exponential distribution does not have a term explicitly related to the variance because there is only one parameter for the exponential distribution (the mean). It is interesting to note that none of the expressions for the GEE include the erodability coefficient β or the slope exponent n. However, equations (17) and (20) do show that Q_p depends upon m and Q_c.

[12] To understand the impacts of the exponent m and critical discharge Q_c on the GEE, we consider a hypothetical location that drains a relatively small area in a humid climate. The mean precipitation rate during storms was found from *Hawk* [1992] and actually applies to Allentown, Pennsylvania ($\overline{P}$ = 1.43 mm/hr), and the drainage area A is arbitrarily selected to be 1 km^2. Thus the mean discharge during a storm would be $\overline{Q} = \overline{P}A = 0.397$ m^3/s. For the lognormal distribution, three arbitrary values were assigned for σ_y: 0.8, 1.0, and 1.2, which correspond to C_Q = 0.95, 1.32, and 1.80, respectively. For comparison σ_y implied by the exponential distribution and *Hawk* [1992] is 0.83. *Hawk* [1992] also gives the mean storm duration and interstorm period for Allentown ($\overline{T}_r$ = 5.42 hrs and $\overline{T}_o$ = 61 hrs). Using the exponential distributions for storm durations and interstorm periods as well as either the exponential distribution or lognormal distribution of discharges during the events, we simulated a discharge record for 1000 years and obtained estimates for the 1-year, 2-year, 5-year, and 10-year events using the Weibull plotting position formula [*Chow et al.*, 1988]. These estimates depend on the values of $\overline{T}_r$ and $\overline{T}_o$ and thus are specific to the geographical location. The discharges are expressed as dimensionless quantities by normalizing by the mean discharge during storm events ($q = Q/\overline{Q}$) and are tabulated in Table 1 for reference.

[13] Figure 1 shows the behavior of the GEE as the exponent m and the critical discharge Q_c are varied. These results were obtained by solving equations (17)

Table 1. Dimensionless Discharges q Associated With Different Return Periods for the Exponential and Lognormal Distributions of Discharge During Storm Events[a]

	Dimensionless Discharge			
Return Period	Exponential Distribution	Lognormal Distribution		
		$\sigma_y = 0.8$	$\sigma_y = 1.0$	$\sigma_y = 1.2$
1 year	2.7	2.6	3.0	3.5
2 years	5.2	5.7	8.0	10.4
5 years	6.3	7.7	12.0	16.4
10 years	7.1	9.2	14.8	21.6

[a]These estimates are specific to climate parameters from Allentown, Pennsylvania.

and (20) numerically. In all figures, the GEE Q_p and the critical discharge Q_c are expressed as dimensionless quantities q_p and q_c, respectively ($q_p \equiv Q_p/\overline{Q}$ and $q_c \equiv Q_c/\overline{Q}$). Figure 1a shows the GEE for the exponential distribution. When the threshold is absent ($q_c = 0$), the GEE increases linearly with increasing m, which is implied by equation (18). When the threshold is large ($q_c \geq 5$), the GEE is almost independent of m and tends toward $q_p = 1 + q_c$ (i.e., $Q_p = \overline{Q} + Q_c$), which indicates that the behavior of fluvial processes after the threshold is exceeded does not affect the GEE. If a 1-year event is empirically determined to be this location's GEE, for example, this return period constrains the value of the threshold but tells us little about the value of m. Figures 1b–1d show the GEE for the lognormal distribution with $\sigma_y = 0.8$, 1.0, and 1.2, respectively. In contrast with the results from the exponential distribution, the GEE increases nonlinearly with increasing m when the threshold is absent (which confirms equation (21)). When a threshold is included, the GEE depends primarily on the value of the threshold when m is small ($0 < m < 2$). When m is large ($m > 3$), the GEE depends primarily on the value of m and is insensitive to the presence of the threshold. Comparing Figures 1b–1d, we see that a larger value of σ_y produces a larger GEE value for any given m and q_c. A larger value of σ_y also produces a more abrupt transition between GEEs controlled by q_c and GEEs controlled by m. It has been previously assumed by many researchers that bedrock detachment is described by a stream power model with an exponent of $m = 1/3$ and a threshold $q_c = 0$. If discharge during storm events also conforms to either the exponential or lognormal distributions considered here, then Figure 1 shows that the GEE has a return period of much less than one year, which is unlikely. In fact, *Tucker* [2004] also argued that the linear stream power model without a threshold is too simplistic for most cases of channel incision.

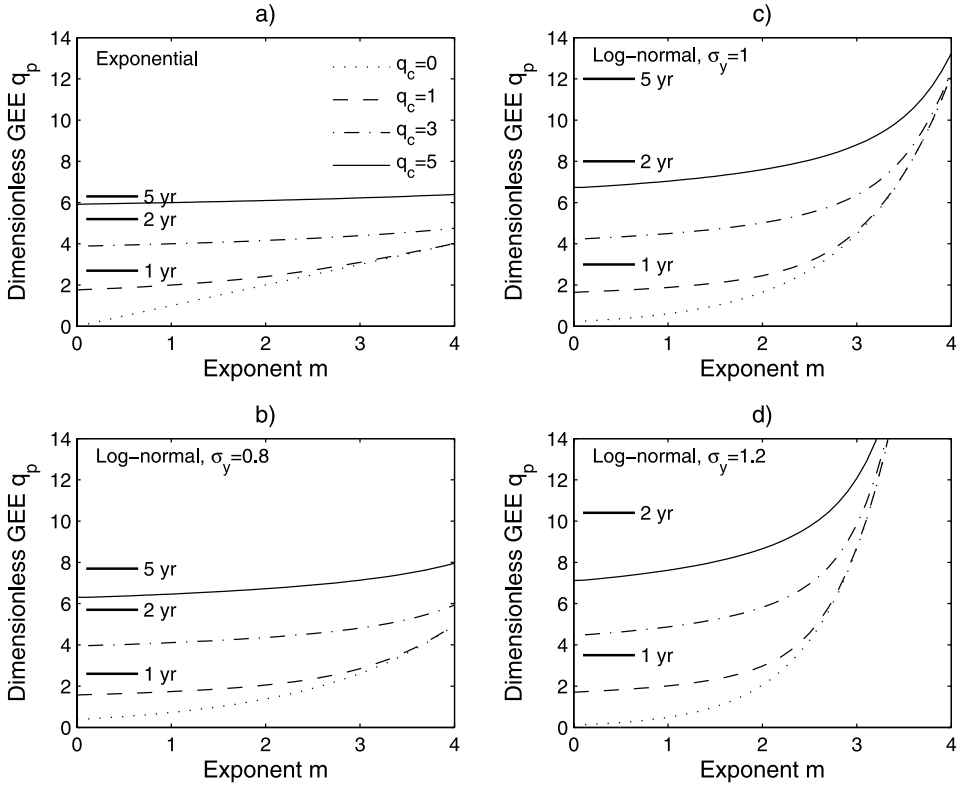

Figure 1. Impacts of exponent on discharge m and dimensionless critical discharge q_c on the dimensionless GEE q_p for (a) the exponential distribution and three lognormal distributions with the standard deviation (b) $\sigma_y = 0.8$, (c) $\sigma_y = 1.0$, and (d) $\sigma_y = 1.2$. The short horizontal lines denote the dimensionless discharges associated with different return periods, which are calculated from the climate parameters of Allentown, Pennsylvania.

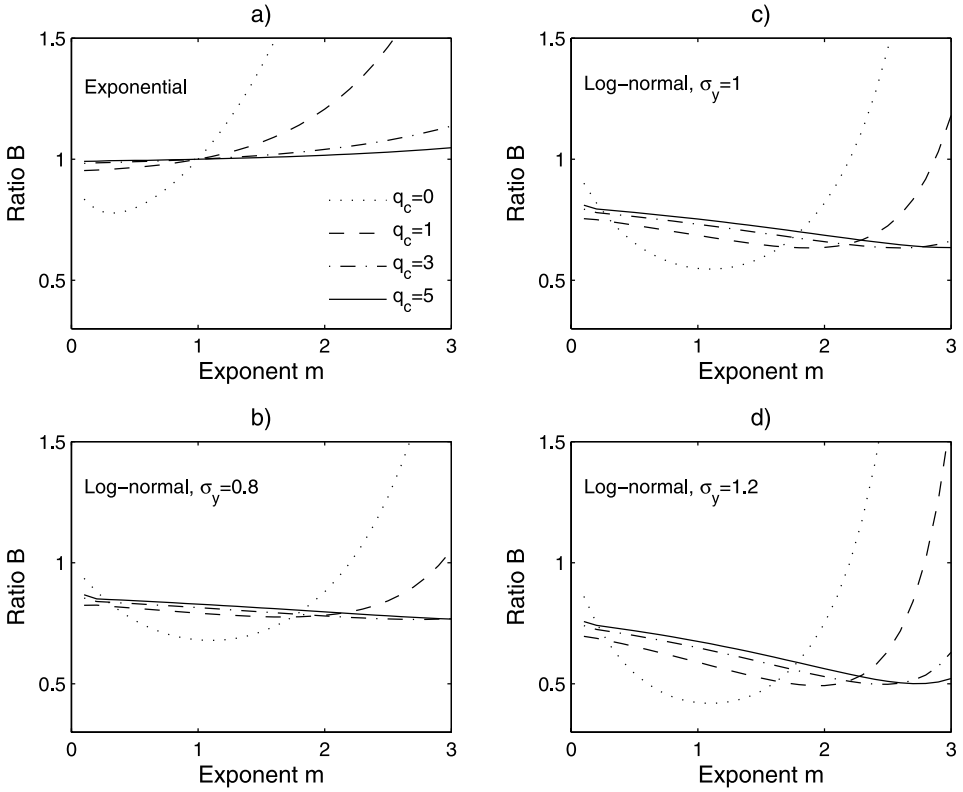

Figure 2. Impacts of m and q_c on the ability of the GEE to reproduce the average erosion rate produced by (a) an exponential distribution and three lognormal distributions with (b) σ_y = 0.8, (c) σ_y = 1.0, and (d) σ_y = 1.2. B is the ratio of the average erosion rate produced by the GEE to that produced by the distribution of discharges.

2.2. Effectiveness of the GEE

[14] By definition the GEE represents the discharge that makes the most important contribution to the fluvial processes over long periods. However, it is not clear whether the GEE can be used in place of the PDF of discharge and obtain the same average erosion rate. This question is important for both numerical modeling of landscape evolution and the use of the stream power model in interpreting field data. For example, if one uses a single effective discharge in a landscape evolution model instead of explicitly accounting for the variability of discharge, is the GEE the correct choice for the effective discharge? Similarly, if an effective discharge is inferred for a field site using the stream power model without explicit consideration of the variability of discharge, is that effective discharge the GEE?

[15] To resolve this issue, the average erosion rate is calculated when either the exponential or lognormal PDF of discharge is used to determine the individual erosion rates and when the GEE alone is used to determine the erosion rates. When the full PDF is used, a discharge Q is first generated from the appropriate $f_Q(Q)$. If $Q > Q_c$, then the erosion rate is calculated as $E = g(Q)$, otherwise no erosion occurs. When the GEE is used in place of the distribution, a discharge Q is still generated from $f_Q(Q)$. If $Q > Q_c$, then the erosion rate is calculated as $E = g(Q_p)$, otherwise no erosion occurs. By using this method, the number of storms producing erosion is the same in both methods. If Q_p is used for every storm event including those below the threshold, then the GEE significantly overestimates the erosion whenever $Q_c > 0$. The performance of the GEE can then be evaluated by calculating the ratio of the two average erosion rates B:

$$B = \frac{\int_{Q_c}^{\infty} g(Q_p) f_Q(Q) dQ}{\int_{Q_c}^{\infty} g(Q) f_Q(Q) dQ} \tag{22}$$

where the numerator describes the average erosion rate produced by the GEE and the dominator describes the average erosion rate produced by the full PDF. If $B = 1$, then the GEE generates the same average erosion rate as the discharges generated from the selected distribution. If $B > 1$, then using the GEE instead of the distribution overestimates the average erosion rate.

[16] For the exponential distribution, equation (22) can be evaluated analytically:

$$B = \frac{\left(Q_p^m - Q_c^m\right) \cdot \exp\left(-Q_c/\overline{Q}\right)}{\overline{Q}^m \Gamma\left(m+1, Q_c/\overline{Q}\right) - Q_c^m \cdot \exp\left(-Q_c/\overline{Q}\right)} \tag{23}$$

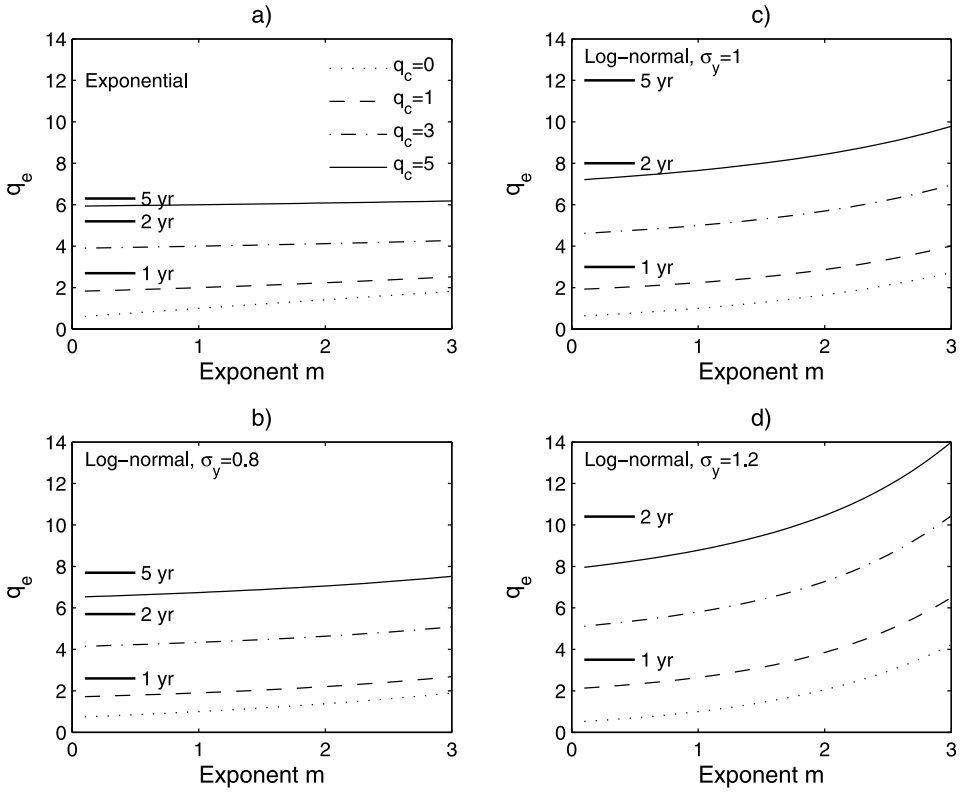

Figure 3. Impacts of m and q_c on the dimensionless effective discharge ($q_e \equiv Q_e/\overline{Q}$) for (a) the exponential distribution and three lognormal distributions with (b) $\sigma_y = 0.8$, (c) $\sigma_y = 1.0$, and (d) $\sigma_y = 1.2$. The short horizontal lines denote the dimensionless discharges associated with different return periods, which are calculated from the climate parameters of Allentown, Pennsylvania.

where $\Gamma(\cdot,\cdot)$ is the incomplete gamma function. Similarly, for the lognormal distribution, one can calculate

$$B = \frac{\left(Q_p^m - Q_c^m\right) \cdot \mathrm{erfc}\left(s_c/\sqrt{2}\right)}{\exp\left(m\mu_y + 0.5m^2\sigma_y^2\right) \cdot \mathrm{erfc}\left(t_c/\sqrt{2}\right) - Q_c^m \cdot \mathrm{erfc}\left(s_c/\sqrt{2}\right)} \tag{24}$$

where erfc(·) is the complementary error function, $s_c \equiv (\ln(Q_c) - \mu_y)/\sigma_y$, and $t_c \equiv [\ln(Q_c) - \mu_y - m\sigma_y^2]/\sigma_y$.

[17] Figure 2a shows the behavior of equation (23) for the exponential distribution, and Figures 2b–2d show the behavior of equation (24) for the lognormal distribution with different variances. For the exponential distribution, the GEE is a suitable effective discharge when $m \approx 1$ or $m \approx 0$. Otherwise, the GEE underestimates the average erosion rate when $m < 1$, and it overestimates the average erosion rate when $m > 1$. As the threshold becomes large, however, the erosion rate produced by the GEE is increasingly similar to the erosion rate from the PDF of discharge. In Figures 2b–2d, the GEE usually underestimates the erosion rate when $m < 2$ and overestimates the erosion rate when $m > 2$. Also, the GEE is generally a poorer representation as the standard deviation of discharge increases. These results demonstrate that while the GEE is the most effective discharge in shaping the fluvial landscape, it is usually not an appropriate substitution for the PDF of discharge.

[18] The appropriate effective discharge can be calculated analytically by setting $B = 1$ and solving for the effective discharge (labeled Q_p in equations (23) and (24)). If we call the correct effective discharge Q_e, then for the exponential distribution:

$$Q_e = \left[\frac{\Gamma\left(m+1, Q_c/\overline{Q}\right)}{\exp\left(-Q_c/\overline{Q}\right)}\right]^{1/m} \overline{Q} \tag{25}$$

and for the lognormal distribution:

$$Q_e = \left[\frac{\mathrm{erfc}\left(t_c/\sqrt{2}\right)}{\mathrm{erfc}\left(s_c/\sqrt{2}\right)}\right]^{1/m} \exp\left(\mu_y + 0.5m\sigma_y^2\right). \tag{26}$$

Figure 3 shows the nondimensional effective discharge ($q_e \equiv Q_e/\overline{Q}$) as a function of m and q_c for the exponential and lognormal distributions. Comparing Figures 1 and 3, we can see that q_e is much different from the GEE in most cases. Most notably, q_e is usually less sensitive to the value of m than q_p. The difference between q_e and q_p is an important result because it implies that the effective discharge inferred from field data with a stream power model that does not consider variability is not equivalent to the GEE. In

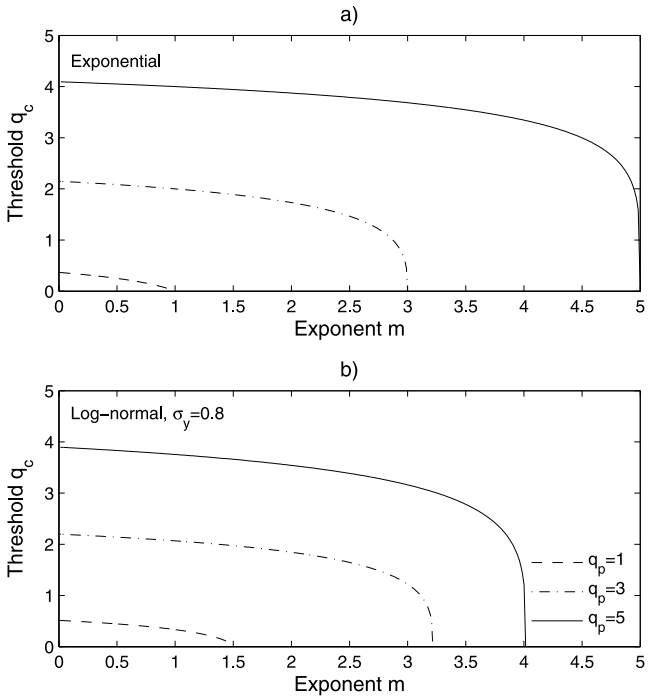

Figure 4. Relationship between m for one fluvial process and q_c for another fluvial process under the condition that the two processes have the same GEE when (a) the exponential distribution is used for discharges and (b) the lognormal distribution with $\sigma_y = 0.8$ is used.

addition, it implies that the appropriate effective discharge for numerical modeling is also not the GEE. However, the result does not suggest that the GEE is unimportant. In fact, the GEE still correctly identifies the most important discharge to the fluvial processes. Figure 3 also implies that the average erosion rate increases with increasing discharge variability when the critical discharge is large (e.g., $q_c = 5$), which is consistent with the results of *Molnar et al.* [2006]. They found that a climate change toward greater aridity leads to larger discharge variability and faster channel incision if the incision is driven by rare large floods.

2.3. Comparison of Bedrock Detachment and Sediment Transport GEEs

[19] On the basis of sections 2.1 and 2.2, we expect that different fluvial processes may have different GEEs because each fluvial process likely has its own exponent m and Q_c. In this section, we evaluate the likelihood that bedrock detachment and sediment transport capacity have the same GEE. We investigate this issue in two ways. First, we assume that the exponent m of one fluvial process and the threshold q_c for the other fluvial process are unknown. If the GEE is the same for both fluvial processes, the unknown threshold q_c can be calculated for any given value of m and q_p by using equations (17) and (20). Figure 4 shows that q_c decreases with increasing m for any given GEE for both the exponential and lognormal distributions. Interestingly, the range of possible m values is limited by the GEE for the two processes if known.

[20] Alternatively, we could assume that the exponent m is known for both fluvial processes but that the thresholds are not known. A relatively small exponent m = 1/3 is used for the bedrock detachment model [*Howard*, 1994; *Tucker and Slingerland*, 1997; *Hancock et al.*, 1998] and a relatively large exponent m = 1.5 is used to calculate sediment transport capacity [*Howard*, 1994]. Given these exponents, the dimensionless critical discharges q_c for bedrock detachment and sediment transport capacity are calculated so that the same GEE is produced for both processes. Figure 5 illustrates that the threshold for the bedrock detachment model is larger than the threshold for the sediment transport model. However, Figure 5 also shows that the two threshold values are quite similar for all GEEs, which conflicts with the expectation that the threshold for bedrock detachment is much larger than the threshold for sediment transport. If thresholds are different for bedrock detachment and sediment transport, it is expected that these two processes respond to different discharges.

3. Analysis With a 1-D Numerical Model

3.1. Model Description

[21] In order to consider the GEE for additional circumstances, a one-dimensional geomorphic model is used to numerically simulate the evolution of a hillslope and channel profile. The hydrologic aspects of this model are nearly identical to those described earlier. Precipitation intensity is simulated according to the exponential distribution in sec-

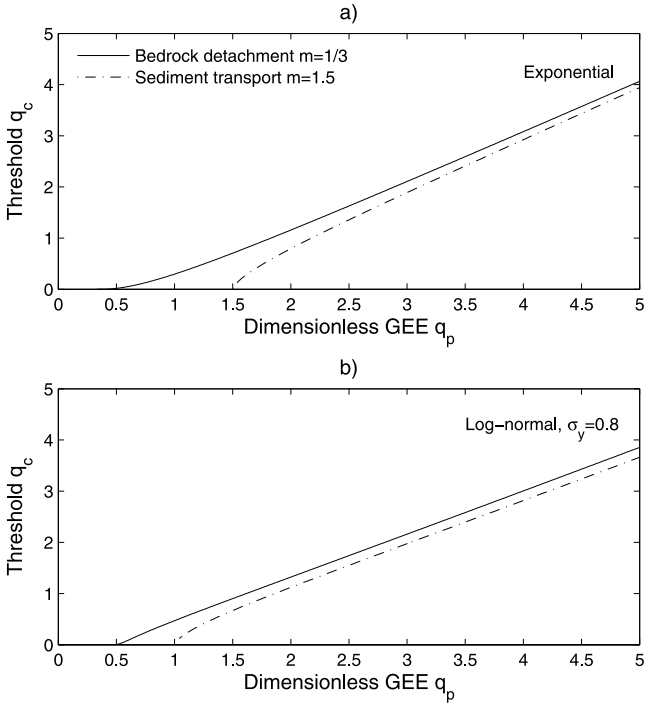

Figure 5. The dimensionless critical discharge for bedrock detachment and sediment transport as a function of the dimensionless GEE if the discharge distribution follows (a) the exponential distribution and (b) the lognormal distribution with $\sigma_y = 0.8$.

Table 2. Parameters Used in the 1-D Hillslope and Valley Profile Model

Parameter	Value
Domain	
Domain size	50
Grid cell size	40 m
Rainfall Model	
Mean rainfall intensity $\overline{P}$	1.43 mm/hr
Mean rainfall duration $\overline{T}_r$	5.42 hrs
Mean interstorm duration $\overline{T}_o$	61 hrs
Detachment-Limited Model	
Base level fall rate U	0.001 m/yr
Coefficient of bedrock detachment β	0.0015 $yr^{-2/3}$
Exponent m	1/3
Exponent n	2/3
Threshold for detachment Φ	0.0 m/yr, 0.012 m/yr, 0.045 m/yr
Diffusivity k_d	6 m^2/yr, 4 m^2/yr, 2 m^2/yr
Transport-Limited Model	
Base level fall rate U	0.001 m/yr
Coefficient of sediment transport β	0.0005 $m^{-1.5}yr^{0.5}$
Exponent m	1.5
Exponent n	2.0
Threshold for transport Φ	0.0 m^3/yr, 5×10^4 m^3/yr, 2×10^5 m^3/yr
Diffusivity k_d	20 m^2/yr, 6 m^2/yr, 3 m^2/yr

tion 2.1 (equation (9)), and the storm durations and interstorm periods also are simulated using exponential distributions. To calculate the discharge at any point i along the profile, it is assumed that

$$A_i = L_i^2 \tag{27}$$

where L_i is the distance of the location from the divide. This expression assumes the profile occurs in a self-similar watershed [*Mandelbrot*, 1983; *Veneziano and Niemann*, 2000; *Hack*, 1957], and it neglects the effects of channel sinuosity and the discrete occurrences of channel junctions [*Tucker and Slingerland*, 1994; *Veneziano and Niemann*, 2000]. Therefore the water discharge Q_i during a storm can be written as

$$Q_i = PA_i = PL_i^2 \tag{28}$$

where P is a rainfall rate generated according to the exponential distribution.

[22] Two distinct models are used to simulate the evolution of the profile. The first includes the so-called detachment-limited expression for erosion [i.e., *Moglen and Bras*, 1995]. The governing equation for the detachment-limited model is

$$\frac{\partial z}{\partial t} = U + k_d \frac{\partial^2 z}{\partial x^2} - (\beta Q^m S^n - \Phi) \tag{29}$$

where z is elevation, t is time, U is the rate of base level fall, k_d is a diffusivity parameter, and x is the horizontal coordinate. The first term on the right side describes both tectonic uplift and base level fall as being constant in time and uniform in space, and it acts to raise the profile relative to the outlet, which is held fixed. The second term represents diffusive hillslope processes including rain splash and soil creep. The third term describes fluvial detachment. Because this term depends on the discharge, it occurs intermittently. This model assumes that detached material is immediately removed from the basin and is not deposited at downstream points. This model is perhaps the simplest one with an erosion threshold that will produce a profile with both hillslope and valley portions.

[23] The second model we consider is the transport-limited model. This model includes base level fall and hillslope processes as before, but it also assumes that fluvial processes can readily detach material so that the transport capacity of the flow limits the fluvial erosion. The governing equation for this model is

$$\frac{\partial z}{\partial x} = U + k_d \frac{\partial^2 z}{\partial x^2} - \nabla \cdot Q_s \tag{30}$$

where $\nabla \cdot$ denotes the spatial divergence and Q_s denotes the sediment transport rate. In this model, the stream power expression is assumed to apply to the sediment transport capacity. Because the model assumes transport-limited conditions, the actual sediment transport rate is always equal to the sediment transport capacity. Thus

$$Q_s = \beta Q^m S^n - \Phi. \tag{31}$$

[24] Three simulations were run for both the detachment-limited and the transport-limited models using different thresholds. The initial river profile has an extremely slight slope toward the outlet to define the direction of flow, and the distance from the divide to the outlet is arbitrarily set to 2 km. Water and sediment leave the system only through the outlet. The profiles are allowed to evolve from the initial state to a steady state where the denudation processes balance the rate of base level fall. The diffusivity k_d is

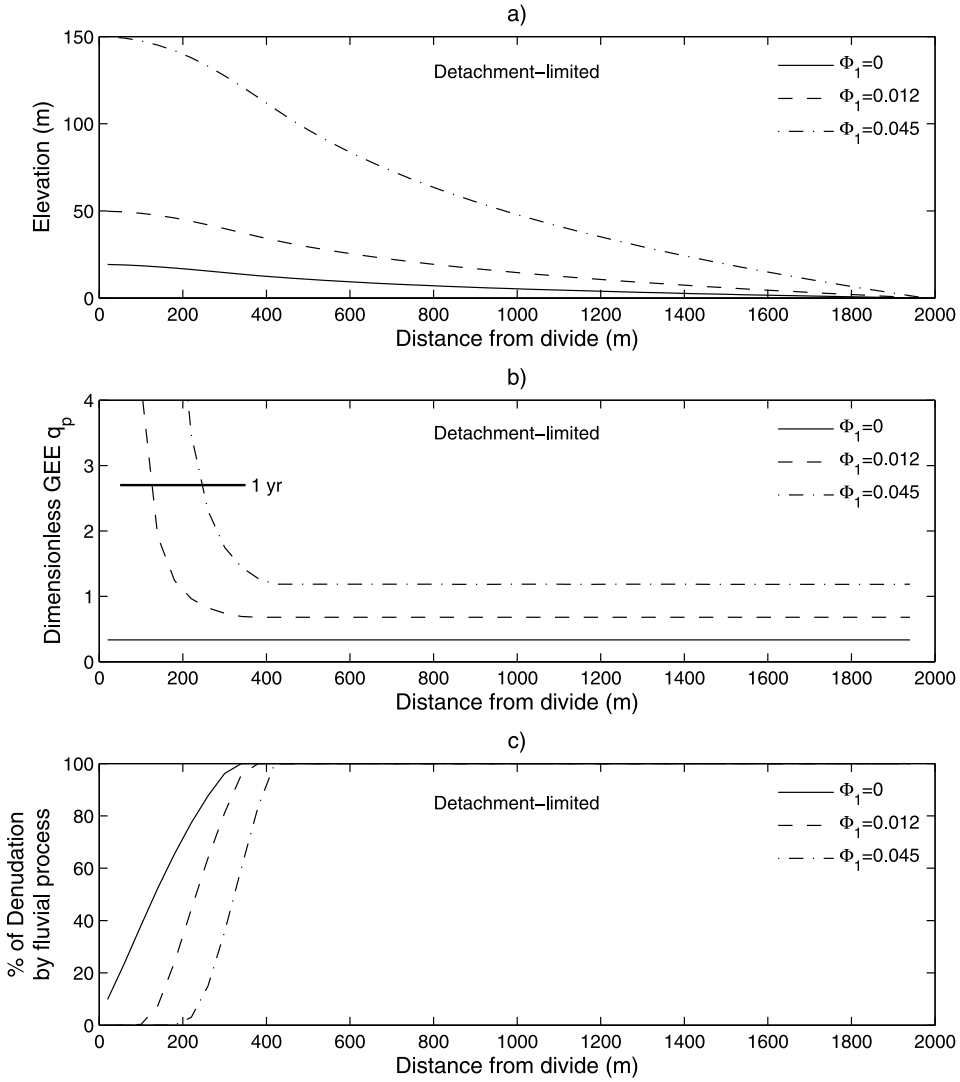

Figure 6. (a) Combined hillslope and valley profiles generated by the detachment-limited model with three different thresholds, (b) the dimensionless GEE along these profiles, and (c) the contribution of fluvial detachment to the total denudation. The short horizontal line in Figure 6b denotes the dimensionless discharge associated with a 1 year event.

varied for each simulation to ensure that all steady state profiles have approximately the same hillslope size. The threshold values (Φ) are 0.0, 0.012, and 0.045 m/yr for the detachment-limited simulations and 0.0, 5×10^4, and 2×10^5 m^3/yr for the transport-limited simulations. Other parameters for the simulations are given in Table 2.

3.2. GEE of a Subdominant Fluvial Process

[25] Figure 6 shows how the threshold for bedrock detachment affects the steady state profile and the dimensionless GEE. The dimensionless GEE at each location is calculated using the location's contributing area and slope and equation (17). In Figure 6a, the steady state river profile increases in elevation with an increasing threshold value because a larger threshold requires larger slopes for the fluvial erosion to balance the base level fall. Figure 6b shows that the downstream portion of the profile has a constant dimensionless GEE along its length, which also implies a constant return period for the GEE in this segment. This portion of the profile roughly corresponds to the concave portion in Figure 6a, and Figure 6c shows that fluvial detachment is the dominant geomorphic process for this segment. The constant GEE in the fluvial section results from the fact that the dimensionless critical discharge q_c is constant. In particular,

$$q_c = \frac{Q_c}{\overline{Q}} = \frac{[\Phi/(\beta S^n)]^{1/m}}{\overline{P}A} = \left(\frac{\Phi}{\beta \overline{P}^m A^m S^n}\right)^{1/m} = \text{const} \qquad (32)$$

where the term $A^m S^n$ is constant along the steady state detachment-limited river profile [*Howard*, 1994; *Willgoose*, 1994]. On the basis of Figure 1, the GEE is determined from only the dimensionless critical discharge q_c and the exponent m, which is also constant. Figure 6b also shows

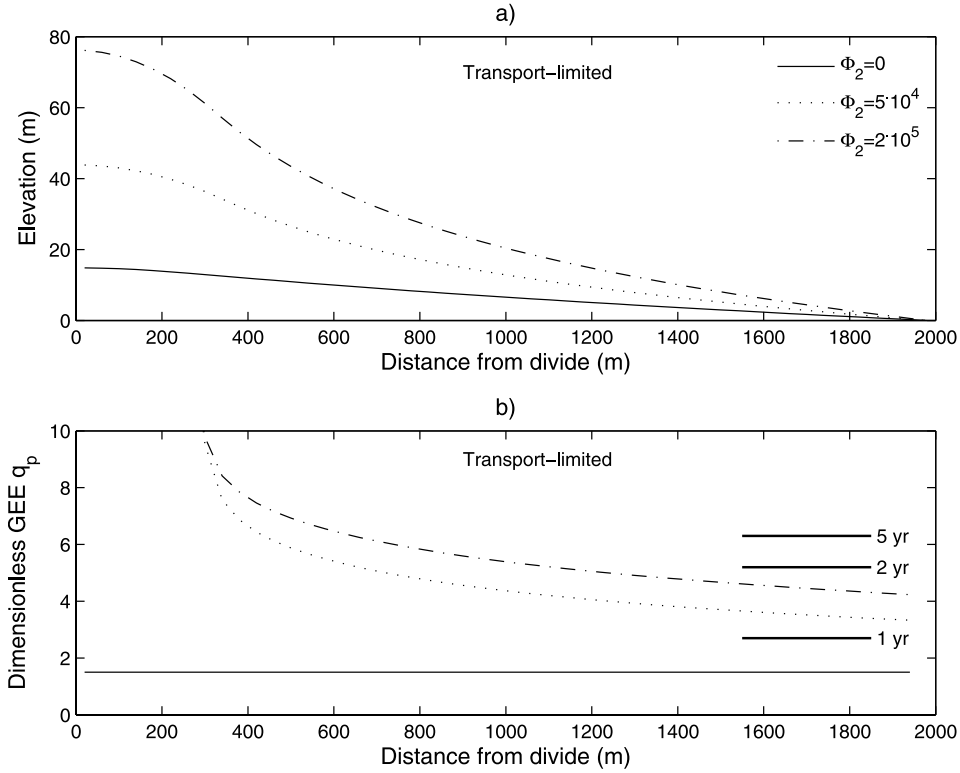

Figure 7. (a) Steady state profiles generated by the transport-limited model with three different thresholds and (b) the dimensionless GEE along these profiles. The short horizontal lines in Figure 7b denote the dimensionless discharges associated with different return periods.

that the GEE diverges from the constant value on the hillslope when a threshold is present in the detachment-limited model. In this portion of the profile, the diffusive process is dominant, but the fluvial process still occurs. The GEE in the hillslope portion is the discharge that contributes the most to the long-term fluvial incision. Interestingly, the most effective discharges on the hillslope are more infrequent than the most effective discharges in the valley. Figure 6b shows that the dimensionless GEE on the hillslope reaches twice the value in the valley when the fluvial process contributes about 20% of the total denudation. Thus the fluvial process is of secondary importance but not trivial when the GEE begins to diverge substantially from the GEE in the channel.

3.3. Spatial Variations of the GEE at Equilibrium

[26] Figure 7 shows how the threshold for sediment transport affects the steady state profile and the dimensionless GEE along the profile. The dimensionless GEE is calculated according to equation (17). As expected, the steady state profile increases in elevation with an increasing threshold value in Figure 7a. In Figure 7b, the lowest transport-limited profile has a constant dimensionless GEE because the threshold is zero. However, the upper two profiles have a decreasing dimensionless GEE as one moves downstream, which suggests that different points on the profile have GEEs with different return periods. In the transport-limited steady state condition, each point in the domain is responsible for removing the sediment produced locally as well as the sediment produced upstream. Thus the geomorphic system evolves such that local slope increases upstream more gently than it does for the detachment-limited condition. In other words, for a given values of m and n, the transport-limited model produces a profile with lower concavity than the detachment-limited model [*Howard*, 1994; *Willgoose*, 1994]. The fact that the GEE varies as one moves downstream can be demonstrated by considering q_c again. For the transport limited model, one can show that

$$q_c = \frac{Q_c}{\overline{Q}} = \frac{[\Phi/(\beta S^n)]^{1/m}}{\overline{P}A} = \left(\frac{\Phi}{\beta \overline{P}^m A^{m-1} S^n}\right)^{1/m} A^{-1/m}. \quad (33)$$

The dependence on contributing area in the final term indicates that q_c varies along the profile. While the mean discharge $\overline{Q}$ increases linearly with an increasing contributing area, the critical discharge Q_c increases much slower with the increasing contributing area. Thus the dimensionless GEE will vary as well. This result is consistent with field observations suggesting that the return period of the GEE for sediment transport decreases as the contributing area increases [*Andrews*, 1980]. However, these field observations did not necessarily consider streams at steady state.

3.4. GEE During Transient Responses

[27] Knickpoint migration occurs when a geomorphic system is subjected to a change in external forcing such

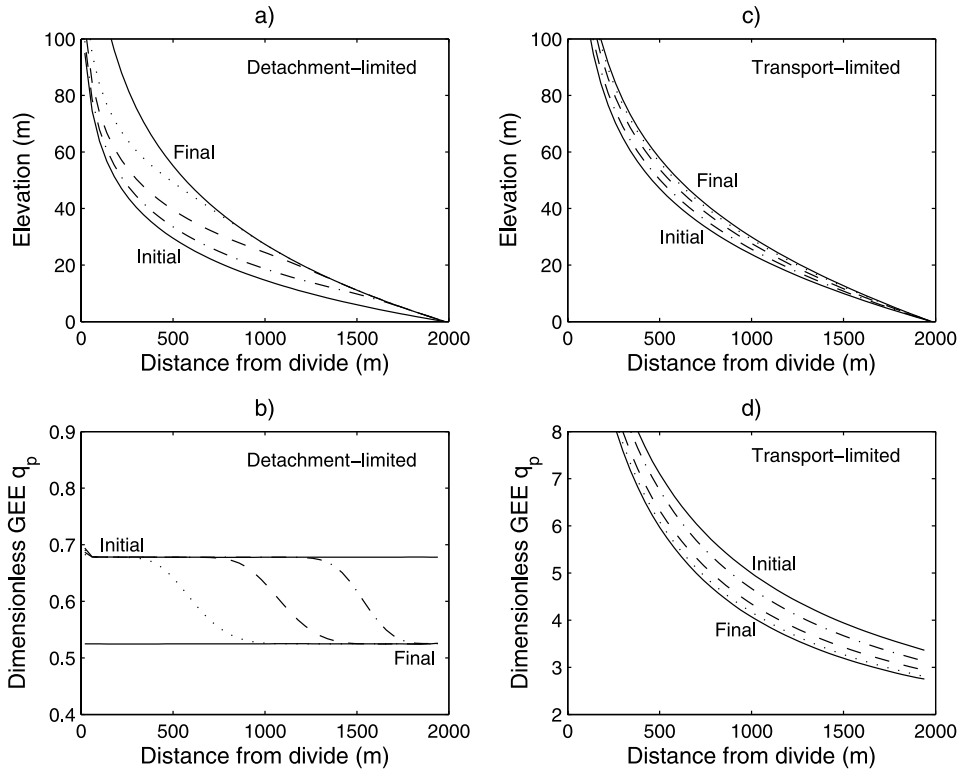

Figure 8. (a) Transient river profiles and (b) associated dimensionless GEEs for the detachment-limited model and (c) transient river profiles and (d) associated dimensionless GEEs for the transport-limited model. The top and bottom solid curves denote the initial and final steady state river profiles, respectively. The other three curves denote transient profiles.

as an abrupt change in the rate of base level fall. The knickpoint is the point on the river profile that separates a downstream section, which has mostly adjusted to the new conditions, and an upstream portion, which mostly reflects the previous conditions. Results from the earlier sections suggest that the GEE may be different for the upstream and downstream portions of a stream during such a transient.

[28] The propagation of a knickpoint is simulated using the 1-D geomorphic models described above. To focus on the behavior in the valleys, hillslope processes are not included in either model in this case. The river profile begins in steady state with a small rate of base level fall (1 mm/yr), then the rate of base level fall is doubled (2 mm/yr). The GEE is calculated along the river profile for the transient states according to equation (17).

[29] Figure 8 demonstrates how the profile and the dimensionless GEE respond to the increase in the rate of base level fall for both the detachment-limited and transport-limited conditions. For the detachment-limited condition, Figure 8a clearly shows the propagation of the knickpoint, and Figure 8b shows that the dimensionless GEE has different values along the profile. The q_p value above the knickpoint is equivalent to q_p of the initial steady state profile, while the q_p value below the knickpoint is determined from the final steady state condition. The points near the knickpoint itself have q_p values between the upstream and downstream values. The transition of the dimensionless GEE around the knickpoint is also affected by the slope exponent n in equation (29), which has been shown to affect the shape of the knickpoint itself [*Tucker and Whipple*, 2002]. For the transport-limited case in Figure 8c, there is no clear knickpoint because the transport-limited condition makes the river profile respond more uniformly. In this case, Figure 8d illustrates that the dimensionless GEE shifts more or less simultaneously from the initial to final values at all locations along the profile.

4. Analysis With a 2-D Numerical Model

[30] The 1-D geomorphic model described above uses a simple representation of basin hydrology (i.e., $Q = PA$), which implies that streamflow generation occurs uniformly across the basin and that the temporal variation of discharge matches the temporal variation of precipitation exactly. While these approximations are commonly used in landscape evolution analysis and modeling, they are both unlikely to occur for most landscapes [*Tucker and Bras*, 2000; *Tucker*, 2004; *Huang and Niemann*, 2006]. Given the results in the previous sections, one might expect that a more detailed description of basin hydrology could produce further spatial variations of the dimensionless GEE and thus the return period of the GEE. To consider the role of streamflow generation processes, a more detailed hydrologic model is imbedded in a 2-D detachment-limited landscape evolution model.

Table 3. Parameters Used in the 2-D Detachment-Limited Landscape Evolution Model

Parameter	Value
Domain	
Domain size	50 × 50
Grid cell size	40 m
Aquifer thickness	2.4 m
Precipitation Model	
Mean rainfall intensity $\overline{P}$	1.43 mm/hr
Mean rainfall duration $\overline{T}_r$	5.42 hrs
Mean interstorm duration $\overline{T}_o$	61 hrs
Geomorphic Model	
Base level fall rate U	0.001 m/yr
Hillslope diffusivity k_d	0.2 m^2/yr
Exponent m	1/3
Exponent n	2/3
Coefficient for detachment β	0.0025 $yr^{-2/3}$
Threshold for detachment Φ	0.0125 m/yr

4.1. Model Description

[31] The geomorphic processes included in the model are the rate of base level fall, denudation by hillslope processes, and detachment by flowing water. The governing equation for the geomorphic model is the same as equation (29), but it is applied to a two-dimensional horizontal grid. Precipitation events occur according to a stochastic process where the intensity, duration, and interstorm periods are determined from exponential distributions as described earlier. However, now a specified infiltration capacity partitions the precipitation between infiltration excess surface runoff and infiltration. Infiltrated water contributes to groundwater, whose movement is simulated using a dynamic depth-integrated model for a shallow, homogeneous, isotropic, and unconfined aquifer [*Dupuit*, 1863]. Groundwater discharge occurs when the water table reaches the surface, and saturation excess surface runoff occurs where precipitation falls on locations where the water table is at the surface. For a more detailed explanation of this model, see *Huang and Niemann* [2006] who applied this combined hydrologic/geomorphic model to the WE-38 experimental watershed near Allentown, Pennsylvania.

[32] Four simulations were run using the same parameters except for the infiltration capacity, which was varied to control the contribution of saturation excess runoff and groundwater discharge to the basin's hydrologic and geomorphic behavior. The assigned infiltration capacities were 0, 0.3, 1.0, and 2.3 mm/hr, which result in 0%, 20%, 50%, and 80% of precipitation infiltrating to groundwater, respectively. Other parameters are provided in Table 3. The simulations began with an essentially flat topography and

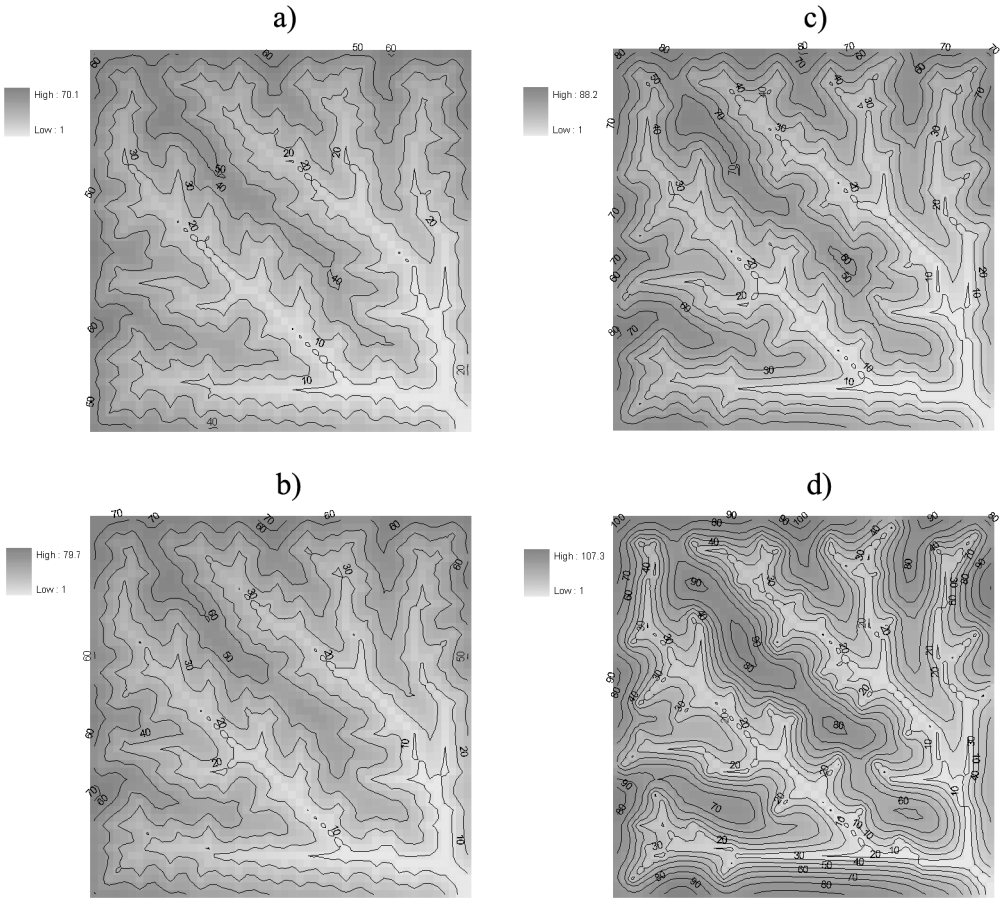

Figure 9. Contour plots of elevation showing the steady state topographies generated by a detachment-limited model with an infiltration capacity of (a) 0 mm/hr, (b) 0.3 mm/hr, (c) 1.0 mm/hr, and (d) 2.3 mm/hr.

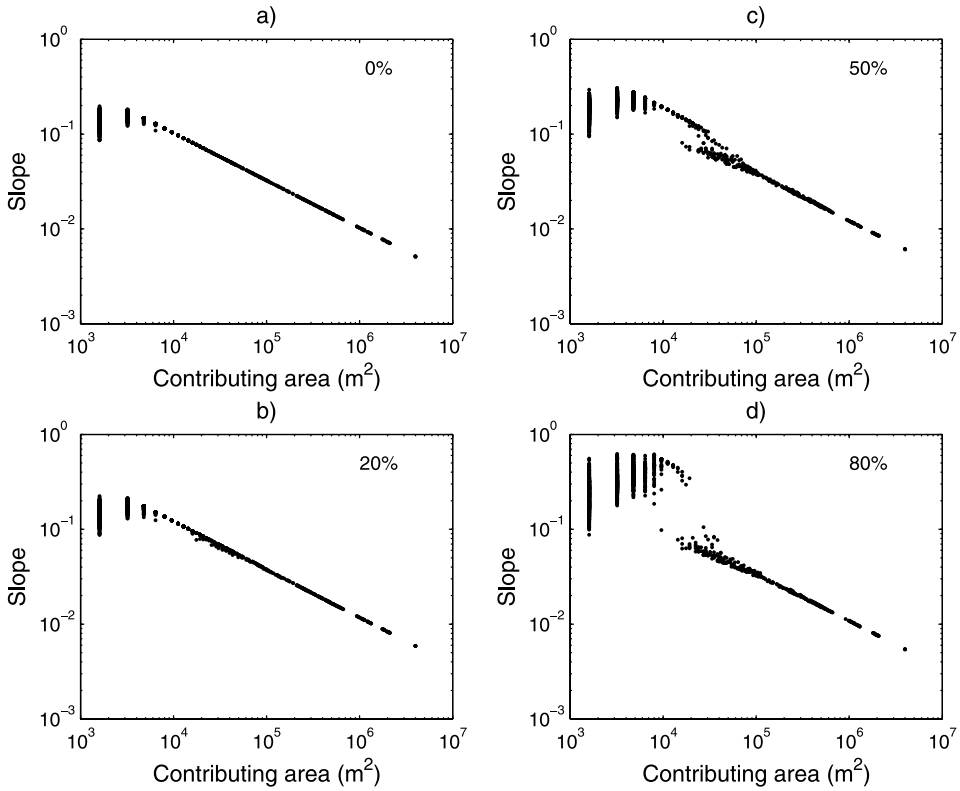

Figure 10. Slope-area relationships for the steady state topographies generated with infiltration capacities of (a) 0 mm/hr, (b) 0.3 mm/hr, (c) 1.0 mm/hr, and (d) 2.3 mm/hr. The percentage given in each plot indicates the portion of the precipitation that infiltrates to the groundwater.

progressed to steady state, which is the condition that is analyzed.

[33] For these simulations, the GEE must be calculated in a different manner than in sections 2 and 3 because both the mean discharge and the distribution of discharge are expected to vary in space. Therefore the GEE was determined from Monte Carlo simulations. After reaching steady state, the model was run for a period of 1000 years, which represents a sample from the probability distribution of discharges. The average detachment rate during every storm and the following interstorm period was calculated at all locations in the watershed. Then, the total erosion produced by discharges within small specified intervals was calculated. The total erosion for each range of discharge indicates the contribution of that range to the total erosion at the location. The GEE can be identified from the discharge range that has the greatest contribution to the total erosion. This method to determine the GEE is very similar to the one typically used in the field [e.g., *Andrews*, 1980].

4.2. GEE With Spatially Variable Runoff Production

[34] Figure 9 shows the steady state topographies generated by the 2-D geomorphic model when different infiltration capacities are used. As the infiltration capacity increases, the basin relief increases and a more abrupt transition between the hillslopes and valleys is observed. When the infiltration capacity is large (>2.3 mm/hr), the fluvial erosion is focused in the valleys and not on the hillslopes, which produces steep valley sidewalls. This behavior occurs because the water table remains below the land surface of the hillslopes during most rainfall events, so little overland flow is available for detachment at these locations. In contrast, the valleys have continuous flows from groundwater discharge and the surface runoff from storm events, which allows continual detachment. Figure 10 shows the slope-area relationships for these topographies. When the infiltration capacity is zero, the slope-area relationship in the valleys is a straight line in the log-log coordinate system. As the infiltration capacity increases, the slope has a more irregular relationship with contributing area. When the infiltration capacity is large (e.g., Figure 10d), the slopes are separated into two distinct groups. The upper group corresponds to hillslope locations, which have larger slopes, and the lower group corresponds to valley locations, which have smaller slopes. A similar behavior was observed by *Tucker and Bras* [1998] using the wetness index [*Beven and Kirkby*, 1979] to simulate saturation excess runoff production.

[35] Figure 11 shows the dimensionless GEE as a function of contributing area for steady state topographies. In Figure 11a, the infiltration capacity is zero, so the results simply confirm that the 1-D results in Figure 6b also apply to a 2-D landscape. As expected, the dimensionless GEE is constant for the valleys and increases for the hillslopes. As the infiltration capacity increases in Figures 11b–11d, the pattern of streamflow generation becomes nonuniform, so

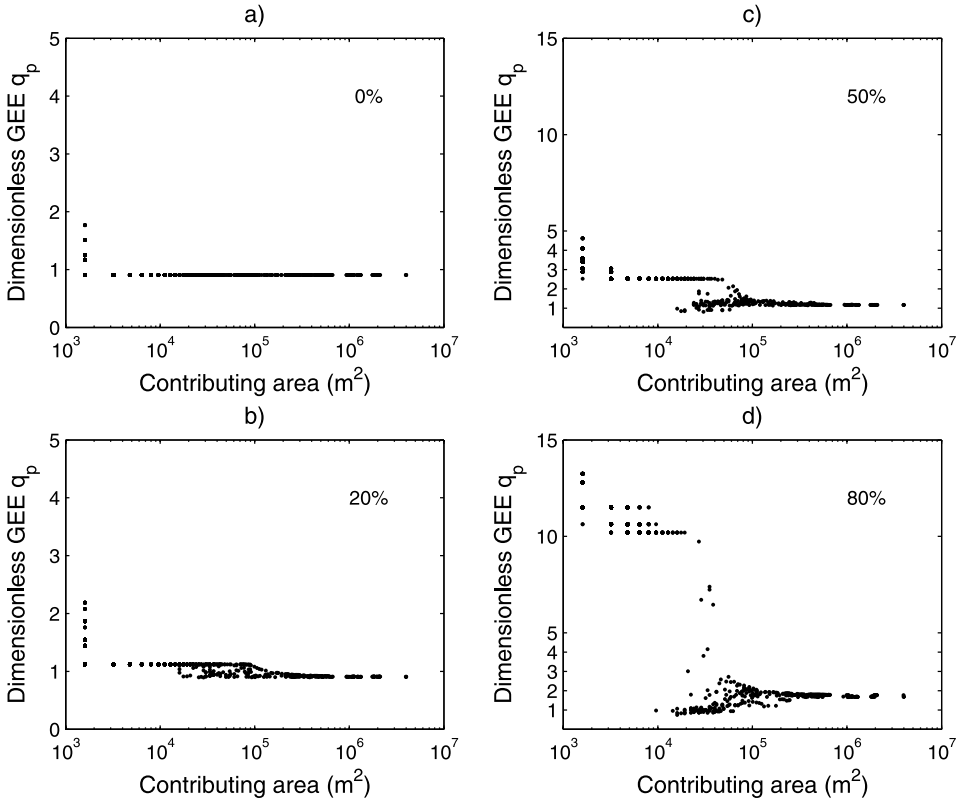

Figure 11. Variation of the dimensionless GEE with contributing area for the steady state topographies generated with infiltration capacities of (a) 0 mm/hr, (b) 0.3 mm/hr, (c) 1.0 mm/hr, and (d) 2.3 mm/hr. The percentage given in each plot indicates the portion of the precipitation that infiltrates to the groundwater.

the dimensionless GEE becomes more variable in the watershed. Figure 11c exhibits four distinct types of locations. When A is less than 4×10^3 m^2, q_p tends to be very large. These locations correspond to hillslope locations that are dominated by diffusive processes. Here, the GEE is similar to the GEE for the hillslopes in Figures 6b and 11a. When A ranges from 4×10^3 m^2 to 4×10^4 m^2, numerous points have a dimensionless GEE at about 2.5. These points correspond to ephemeral channels whose discharge is dominated by infiltration excess runoff. q_p is large for these points because they tend to be groundwater recharge locations. Thus the infiltration capacity is similar to a threshold that must be exceeded before overland flow and detachment can occur. A third group of points with A between 1×10^4 m^2 and 2×10^5 m^2 has variable values of q_p that tend to fall below 2.5. The GEE at these locations is lower than the GEE for other points with similar contributing area because these tend to be groundwater discharge locations. When $A > 2 \times 10^5$ m^2, q_p is constant at a value slightly above one. These points correspond to the perennial channels, which mainly convey discharge from locations upstream. The four zones identified in Figure 11c are more distinct with larger infiltration capacities mainly because the dimensionless GEE of the infiltration excess ephemeral channels tends to increase with increasing infiltration capacity. The dimensionless GEE in the perennial channels also increases with an increasing infiltration capacity because discharges tend to be more distributed in time due to the slow release of groundwater.

5. Discussion and Conclusions

[36] The objective of this paper was to investigate the behavior of the GEE when a stream power model with a threshold is used to describe the detachment of bedrock and the transport of sediment. The main conclusions and their implications are listed below.

[37] 1. When either bedrock detachment or sediment transport is described by a stream power model, both the threshold and the exponent on discharge m can have significant impacts on the GEE. When $m < 2$, the magnitude of the GEE mainly depends on the threshold, and when $m > 2$, the GEE mainly depends on the exponent. The mean discharge is the GEE only when the stream power model has a linear dependence on discharge and a threshold of zero. Given that the available estimates of m for bedrock detachment and sediment transport are consistently at or below two [*Howard*, 1994; *Tucker and Slingerland*, 1997; *Hancock et al.*, 1998], it is most probable that the threshold controls the return period of the GEE.

[38] 2. The single "effective" discharge that produces the same average erosion rate as the PDF of discharge is usually not the GEE. Among the cases considered, the GEE is only an adequate approximation when the distribution of dis-

charge is exponential and $m \approx 0$, $m \approx 1$, or the threshold is large. This result suggests that models describing the long-term effects of bedrock detachment and sediment transport capacity cannot be driven by the GEE alone. This result also has implications for the analysis of field data. In particular, if one derives an effective discharge using a stream power model that does not consider variability of discharge, then this effective discharge is not the GEE.

[39] 3. For a steady state profile, the return period of the GEE is larger on the hillslope where a diffusive process is dominant than it is in the valley where the fluvial process is dominant if a threshold is present. This result implies that the GEE can be different between different locations in a basin depending on whether the water-driven erosion process is the dominant process. It also suggests that estimates of the GEE from channel locations cannot be used as estimates of the GEE in hillslope locations.

[40] 4. Steady state river profiles generated by the detachment-limited model exhibit a constant GEE throughout the channels, but the steady state topography generated by the transport-limited model shows a decreasing dimensionless GEE with increasing contributing area. This result implies that the return period of the GEE upstream is greater than the return period of the GEE downstream. It also suggests that if the random discharges increase linearly with drainage area, then the GEE does not usually increase linearly with drainage area.

[41] 5. When a detachment-limited profile is responding to a change in the rate of base level fall, different dimensionless GEE values are observed upstream and downstream of the knickpoint. For a transport-limited profile, the dimensionless GEE is updated more or less simultaneously throughout the profile. This behavior is important because it suggests that the most important discharge for points in steady state conditions can be different than the most important discharge for points in transient conditions.

[42] 6. Spatial variation in the generation of streamflow also affects the magnitude of the dimensionless GEE in a steady state basin. When saturation excess runoff and groundwater discharge become more important due to a larger specified infiltration capacity, the dimensionless GEE tends to increase for groundwater recharge locations and increase slightly for groundwater discharge locations. Thus nonuniform runoff production mechanisms can produce further spatial variations in the return period of the GEE.

[43] **Acknowledgments.** We gratefully acknowledge financial support from the U.S. Army Research Office Terrestrial Sciences program. We are also indebted to Greg Tucker, Alex Densmore, Robert Anderson, and an anonymous reviewer, who provided helpful suggestions for this manuscript.

References

Anderson, R. S. (1994), Evolution of the Santa Cruz Mountains, California, through tectonic growth and geomorphic decay, *J. Geophys. Res.*, *99*(B10), 20,161–20,179.

Andrews, E. D. (1980), Effective and bankfull discharges of streams in the Yampa River basin, Colorado and Wyoming, *J. Hydrol.*, *46*, 311–330.

Ang, A. H.-S., and W. H. Tang (1975), *Probability Concepts in Engineering Planning and Design*, vol. I, *Basic Principles*, John Wiley, New York.

Ashmore, P. E., and T. J. Day (1988), Effective discharge for suspended sediment transport in streams of the Saskatchewan River basin, *Water Resour. Res.*, *24*, 864–870.

Bagnold, R. A. (1954), *The Physics of Wind Blown Sand and Desert Dunes*, CRC Press, Boca Raton, Fla.

Baker, V. R. (1977), Stream-channel response to floods, with examples from central Texas, *Geol. Soc. Am. Bull.*, *88*(8), 1057–1071.

Benson, M. A., and D. M. Thomas (1966), A definition of dominant discharge, *Bull. Int. Assoc. Sci. Hydrol.*, *11*, 76–80.

Beven, K. J., and M. J. Kirkby (1979), A physically based, variable contributing area model of basin hydrology, *Hydrol. Sci. Bull.*, *24*(1), 43–69.

Chow, V. T. (1954), The log-probability law and its engineering applications, *Proc. Am. Soc. Civ. Eng.*, *80*, 1–25.

Chow, V. T., D. R. Maidment, and L. W. Mays (1988), *Applied Hydrology*, McGraw-Hill, New York.

Costa, J. E., and J. E. O'Connor (1995), Geomorphically effective floods, in *Natural and Anthropogenic Influences in Fluvial Geomorphology*, *Geophys. Monogr. Ser.*, vol. 89, edited by J. E. Costa et al., pp. 45–56, AGU, Washington, D. C.

Densmore, A. L., M. A. Ellis, and R. S. Anderson (1998), Landsliding and the evolution of normal-fault-bounded mountains, *J. Geophys. Res.*, *103*(B7), 15,203–15,219.

Doyle, M. W., E. H. Stanley, D. L. Strayer, R. B. Jacobson, and J. C. Schmidt (2005), Effective discharge analysis of ecological processes in streams, *Water Resour. Res.*, *41*, W11411, doi:10.1029/2005WR004222.

Dupuit, J. (1863), *Etudes theoriques et pratiques sur le mouvement des eaux dans les cannaux decouverts et a travers les terrains permeables*, 2nd ed., Dunod, Paris.

Eagleson, P. S. (1978), Climate, soil and vegetation: 2. The distribution of annual precipitation derived from observed storm sequences, *Water Resour. Res.*, *14*, 713–721.

Hack, J. T. (1957), Studies of longitudinal stream profiles in Virginia and Maryland, *U.S. Geol. Surv. Prof. Pap.*, *294-B*, 45–97.

Hancock, G. S., R. S. Anderson, and K. X. Whipple (1998), Beyond power: Bedrock incision process and form, in *Rivers Over Rock: Fluvial Processes in Bedrock Channels*, *Geophys. Monogr. Ser.*, vol. 107, edited by K. J. Tinkler and E. E. Wohl, pp. 35–60, AGU, Washington, D. C.

Hartshorn, K., N. Hovius, W. B. Dade, and R. L. Slingerland (2002), Climate-driven bedrock incision in an active mountain belt, *Science*, *297*, 2036–2038.

Hawk, K. L. (1992), Climatology of station storm rainfall in the continental United States: Parameters of the Bartlett-Lewis and Poisson rectangular pulses models, M. S. thesis, Mass. Inst. of Technol., Cambridge, Mass.

Howard, A. D. (1994), A detachment-limited model of drainage basin evolution, *Water Resour. Res.*, *30*, 2261–2285.

Howard, A. D. (1997), Badland morphology and evolution: Interpretation using a simulation model, *Earth Surf. Processes Landforms*, *22*(3), 211–227.

Howard, A. D. (1999), Simulation of gully erosion and bistable landforms, in *Incised River Channels*, edited by S. Darby and A. Simon, pp. 277–300, John Wiley, Hoboken, N. J.

Howard, A. D., and G. Kerby (1983), Channel changes in badlands, *Geol. Soc. Am. Bull.*, *94*(6), 739–752.

Huang, X., and J. D. Niemann (2006), Modelling the potential impacts of groundwater hydrology on long-term drainage basin evolution, *Earth Surf. Processes Landforms*, in press.

Kirchner, J. W., R. C. Finkel, C. S. Riebe, D. E. Granger, J. L. Clayton, J. G. King, and W. F. Megahan (2001), Mountain erosion over 10 yr, 10 k.y., and 10 m.y. time scales, *Geology*, *29*(7), 591–594.

Kirkby, M. J. (1986), A two-dimensional simulation model for slope and stream evolution, in *Hillslope Processes*, edited by A. D. Abrahams, pp. 204–222, Allen and Unwin, St. Leonards, N. S. W., Australia.

Kirkby, M. J. (1987), Modelling some influences of soil erosion, landslides and valley gradient on drainage density and hollow development, *Catena Suppl.*, *10*, 1–14.

Krumbein, W. C. (1955), Experimental design in the earth sciences, *Eos Trans. AGU*, *36*, 1–11.

Kuczera, G. (1982), Robust flood frequency models, *Water Resour. Res.*, *18*, 315–324.

Lague, D., N. Hovius, and P. Davy (2005), Discharge, discharge variability, and the bedrock channel profile, *J. Geophys. Res.*, *110*, F04006, doi:10.1029/2004JF000259.

Leopold, L. B. (1994), *A View of the River*, Harvard Univ. Press, Cambridge, Mass.

Mandelbrot, B. B. (1983), *The Fractal Geometry of Nature*, W. H., New York.

Miller, A. J. (1990), Flood hydrology and geomorphic effectiveness in the central Appalachians, *Earth Surf. Processes Landforms*, *15*, 119–134.

Moglen, G. E., and R. L. Bras (1995), The importance of spatially heterogenous erosivity and the cumulative area distribution within a basin evolution model, *Geomorphology*, *12*(3), 173–185.

Molnar, P., R. S. Anderson, G. Kier, and J. Rose (2006), Relationships among probability distributions of stream discharges in floods, climate, bed load transport, and river incision, *J. Geophys. Res.*, *111*, F02001, doi:10.1029/2005JF000310.

Montgomery, D. R., and W. E. Dietrich (1992), Channel initiation and the problem of landscape scale, *Science*, *255*, 826–830.

Nash, D. B. (1994), Effective sediment-transporting discharge from magnitude-frequency analysis, *J. Geol.*, *102*, 79–95.

Nolan, K. M., T. E. Lisle, and H. M. Kelsey (1987), Bankfull discharge and sediment transport in northwestern California, in *Erosion and Sedimentation in the Pacific Rim*, edited by R. L. Beschta et al., *IAHS Publ.*, *165*, 439–449.

Paola, C., P. L. Heller, and C. L. Angevine (1992), The large-scale dynamics of grain-size variation in alluvial basins: 1. Theory, *Basin Res.*, *4*, 73–90.

Ritter, D. F. (1988), Landscape analysis and the search for geomorphic unity, *Geol. Soc. Am. Bull.*, *100*(2), 160–171.

Roering, J. J., J. W. Kirchner, and W. E. Dietrich (1999), Evidence for nonlinear, diffusive sediment transport on hillslopes and implications for landscape morphology, *Water Resour. Res.*, *35*, 853–870.

Seidl, M. A., and W. E. Dietrich (1992), The problem of channel erosion into bedrock, *Catena Suppl.*, *23*, 101–124.

Shields, F. D., R. R. Copeland, P. C. Klingeman, M. W. Doyle, and A. Simon (2003), Design for stream restoration, *J. Hydraul. Eng.*, *129*, 575–584, doi:10.1061/ (ASCE)0733-9429 [2003]129:8 (575).

Sichingabula, H. M. (1999), Magnitude-frequency characteristics of effective discharge for suspended sediment transport, Fraser River, British Columbia, Canada, *Hydrol. Processes*, *13*, 1361–1380.

Sklar, L., and W. E. Dietrich (1998), River longitudinal profiles and bedrock incision models: Stream power and the influence of sediment supply, in *Rivers Over Rock: Fluvial Processes in Bedrock Channels*, *Geophys. Monogr. Ser.*, vol. 107, edited by K. J. Tinkler and E. E. Wohl, pp. 237–260, AGU, Washington, D. C.

Tucker, G. E. (2004), Drainage basin sensitivity to tectonic and climatic forcing: Implications of a stochastic model for the role of entrainment and erosion thresholds, *Earth Surf. Processes Landforms*, *29*, 185–205.

Tucker, G. E., and R. L. Bras (1998), Hillslope processes, drainage density, and landscape morphology, *Water Resour. Res.*, *34*(10), 2751–2764.

Tucker, G. E., and R. L. Bras (2000), A stochastic approach to modeling the role of rainfall variability in drainage basin evolution, *Water Resour. Res.*, *36*(7), 1953–1964.

Tucker, G. E., and R. L. Slingerland (1994), Erosional dynamics, flexural isostacy, and long-lived escarpments: A numerical modeling study, *J. Geophys. Res.*, *99*(B6), 12,229–12,243.

Tucker, G. E., and R. L. Slingerland (1997), Drainage basin response to climate change, *Water Resour. Res.*, *33*, 2031–2047.

Tucker, G. E., and K. X. Whipple (2002), Topographic outcomes predicted by stream erosion models: Sensitivity analysis and intermodel comparison, *J. Geophys. Res.*, *107*(B9), 2179, doi:10.1029/2001JB000162.

Veneziano, D., and J. D. Niemann (2000), Self-similarity of multifractality fluvial topography: 2. Scaling properties, *Water Resour. Res.*, *36*, 1937–1951.

Vogel, R. M., J. R. Stedinger, and R. P. Hooper (2003), Discharge indices for water quality loads, *Water Resour. Res.*, *39*(10), 1273, doi:10.1029/2002WR001872.

Whipple, K. X., and G. E. Tucker (1999), Dynamics of the stream-power river incision model: Implications for height limits of mountain ranges, landscape response timescales, and research needs, *J. Geophys. Res.*, *104*(B8), 17,661–17,674.

Willgoose, G. R. (1994), A statistic for testing the elevation characteristics of landscape simulation models, *J. Geophys. Res.*, *99*(B7), 13,987–13,996.

Willgoose, G. R., R. L. Bras, and I. Rodríguez-Iturbe (1991a), A coupled channel network growth and hillslope evolution model: 1. Theory, *Water Resour. Res.*, *27*, 1671–1684.

Willgoose, G. R., R. L. Bras, and I. Rodríguez-Iturbe (1991b), A coupled channel network growth and hillslope evolution model: 2. Nondimensionalization and applications, *Water Resour. Res.*, *27*, 1685–1696.

Willgoose, G. R., R. L. Bras, and I. Rodríguez-Iturbe (1991c), A physical explanation of an observed link area-slope relationship, *Water Resour. Res.*, *27*, 1697–1702.

Wolman, M. G., and R. Gerson (1978), Relative scales of time and effectiveness of climate in watershed geomorphology, *Earth Surf. Processes*, *3*, 189–208.

Wolman, M. G., and J. P. Miller (1960), Magnitude and frequency of forces in geomorphic processes, *J. Geol.*, *68*(1), 54–74.

X. Huang, Department of Civil and Environmental Engineering, Pennsylvania State University, University Park, PA 16802, USA.

J. D. Niemann, Department of Civil Engineering, Colorado State University, Campus Delivery 1372, Fort Collins, CO 80523-1372, USA. (jniemann@engr.colostate.edu)